Structural properties of oxygen-deficient $YBa_2Cu_3O_{7-\delta}$

J. D. Jorgensen, B. W. Veal, A. P. Paulikas, L. J. Nowicki, G. W. Crabtree,
H. Claus,* and W. K. Kwok†
Materials Science Division, Argonne National Laboratory, Argonne, Illinois 60439
(Received 17 July 1989; revised manuscript received 25 September 1989)

The structural properties of oxygen-deficient $YBa_2Cu_3O_{7-\delta}$ have been determined by neutron powder diffraction for $0.07 < \delta < 0.91$. The samples were produced by quenching into liquid nitrogen from controlled oxygen partial pressures at 520 °C, and they exhibit a clearly defined "plateau" behavior of T_c versus δ. Superconductivity disappears at the orthorhombic-to-tetragonal transition that occurs near $\delta = 0.65$. Structural parameters, including the copper-oxygen bond lengths, vary smoothly with δ within each phase but exhibit different behavior in the superconducting and nonsuperconducting phases. These observations are consistent with a model in which superconducting behavior is controlled by charge transfer between the conducting two-dimensional CuO_2 planes and the CuO_x chains, which act as reservoirs of charge.

INTRODUCTION

The dramatic effect of oxygen stoichiometry on the superconducting properties of high-T_c $YBa_2Cu_3O_{7-\delta}$ provides a unique opportunity for exploring the nature of superconductivity in this material. Oxygen-deficient samples prepared by various methods have been extensively studied. Because these samples are metastable, their properties can be dependent on the preparation technique. However, as experimental techniques have improved, a consistent picture of the dependence of the superconducting transition temperature, T_c, on the oxygen stoichiometry has emerged. For the majority of the published data, T_c decreases only slightly from 90 K with increasing δ for $0 < \delta < 0.2$, decreases rapidly for $0.2 < \delta < 0.3$, is nearly constant at approximately 60 K for $0.3 < \delta < 0.5$, and then drops sharply from 60 to 0 K for $0.5 < \delta < 0.6$. The regions $0 < \delta < 0.2$ and $0.3 < \delta < 0.5$, where T_c varies a small amount or is nearly constant, are typically referred to as "plateaus" in T_c.

This "two-plateau" phenomenon has now been observed in samples prepared by such diverse techniques as *in situ* oxygen desorption on a thermogravimetric analysis (TGA) balance while heating in controlled oxygen or nitrogen atmospheres,[1,2] oxygen gettering with Zr foil at 360–520 °C,[3,4] annealing $YBa_2Cu_3O_7$ samples in controlled argon-oxygen mixtures,[5,6] addition of controlled amounts of oxygen to $YBa_2Cu_3O_6$ at high temperature,[7] plasma oxidation of $YBa_2Cu_3O_6$ near room temperature,[8] annealing in oxygen at constant temperature for controlled amounts of time,[9] and quenching from high temperature (400–1000 °C) into liquid nitrogen,[10–13] into cold helium gas,[14] and onto a cold metal block.[15] It appears clear, however, that the occurrence of plateau behavior does depend on sample history and is most pronounced in samples prepared at low temperatures.[3,4] In fact, some high-temperature quenching studies have not shown clear plateau behavior.[16–20]

Several groups have reported results of structural studies of metastable oxygen-deficient $YBa_2Cu_3O_{7-\delta}$. The dependence of the lattice constants on oxygen stoichiometry, and the transition from orthorhombic to tetragonal symmetry with decreasing oxygen have been discussed in several papers (Refs. 1–6, 10, 11, 14, 16, and 18–26). Aside from differences that can be attributed to inaccurate determinations (sometimes only estimates) of the oxygen stoichiometry, most of these studies yield a value of approximately 6.4 (i.e., $\delta = 0.6$) for the oxygen content at the orthorhombic-to-tetragonal (*O-T*) transition.[27] However, some studies report that the orthorhombic phase extends to significantly lower oxygen stoichiometries (e.g., $\delta = 0.8$).[2,3] At the present time it is not clear whether these results represent intrinsic behavior resulting from the orthorhombic phase being stable at lower oxygen compositions for samples equilibrated at low temperature or are simply problems with sample inhomogeneity.

In recent literature, a structural question of greater interest has been the variation of individual atom positions with oxygen stoichiometry. Attention has especially focused on the large variations observed for particular Cu—O bonds. It has been proposed that the Cu—O bonds that link the CuO one-dimensional chains to the CuO_2 two-dimensional planes [i.e., the Cu(1)—O(4) and Cu(2)—O(4) bonds in Fig. 1] offer a sensitive probe of the amount of charge transfer from the chains to the planes.[4,28–32] Unfortunately, previous attempts to specify the Cu—O bond lengths as a function of oxygen content have been based on compilations of bond lengths taken from the literature for samples prepared by a variety of different techniques[4,30–32] or on data for samples quenched from a high temperature that do not show a clear plateau behavior.[17] Clearly, if the sample properties depend on the preparation technique, such an approach is inadequate to determine systematic behavior.

In an attempt to clarify these important questions, we report in this paper the structural properties of a set of oxygen-deficient $YBa_2Cu_3O_{7-\delta}$ samples for which clear

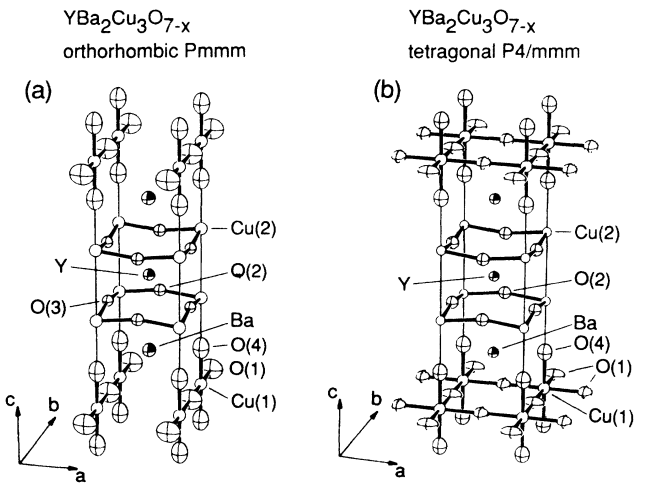

FIG. 1. (a) Orthorhombic and (b) tetragonal structures of $YBa_2Cu_3O_{7-\delta}$. In the tetragonal structure (b) the different atom symbol for the O(1) site is used to indicate that this site is not fully occupied.

plateau behavior is observed. In previous papers we reported on the properties of oxygen-deficient samples quenched into liquid nitrogen from various temperatures as high as 900 °C and a constant oxygen partial pressure of 1 atm.[16,17] The variable quenching temperatures employed in that experiment provided useful information about the properties of oxygen-deficient orthorhombic and tetragonal $YBa_2Cu_3O_{7-\delta}$, but suffered from a rather large amount of scatter in the data, especially for the higher quench temperatures, presumably resulting from oxygen inhomogeneity in the samples. Thus, in that study, it was not clear whether plateau behavior was present. Additionally, the scatter in the structural data was too large to investigate detailed correlations between structural and superconducting properties. In an effort to improve the sample quality, we have performed a second set of experiments for samples quenched into liquid nitrogen from various oxygen partial pressures and a constant temperature of 520 °C. This method produces homogeneous samples of higher quality because of the decreased amount of diffusion during the quenching process. In this paper we report structural properties determined by neutron powder diffraction and Rietveld structure refinement for samples spanning an oxygen composition range of $YBa_2Cu_3O_{6.93}$ to $YBa_2Cu_3O_{6.09}$ and correlate the structural properties to the superconducting properties of the same samples.

SAMPLE PREPARTION AND CHARACTERIZATION

A master batch of $YBa_2Cu_3O_{7-\delta}$ was prepared from powders of Y_2O_3, $BaCO_3$, and CuO. The powders were individually prescreened through 200 mesh, mixed, pressed into pellets, and placed in a platinum crucible for heat treatment. The pellets were heated to 960 °C for 24 h in flowing oxygen for calcining and sintering. The samples were then cooled in air, ground to 200 mesh, remixed, and pressed into pellets that were again sintered at 960 °C in flowing oxygen for 24 h. The temperature was then reduced to 670 °C and held for 24 h followed by cooling to ambient temperature at the rate of 50 °C/h. This master batch showed an inductive onset (or zero resistance) superconducting transition temperature, T_c, of 92 K. The diamagnetic (Meissner) signal was 50% of the maximum at 91 K when measured in a field of 2 Oe. Powder x-ray and neutron diffraction showed no impurity phases except for a few percent Y_2BaCuO_5 ("green phase"). In particular, oxides of copper, which can cause significant errors in weight-loss and iodometric titration measurements, were not observed. The composition of the master batch was determined by iodometric titration,[33,34] averaged over several samples from different parts of the batch, to be $YBa_2Cu_3O_{6.93\pm0.01}$. The uncertainty of ± 0.01 is estimated from the differences between the individual samples.

The oxygen-deficient samples listed in Table I were produced by annealing portions of the master batch at 520 ± 10 °C in a controlled oxygen-argon gas mixture flowing over the sample. Oxygen pressures were monitored with a Thermox I (now Ametek, Inc.) zirconia-cell oxy-

TABLE I. Annealing conditions for oxygen-deficient samples of $YBa_2Cu_3O_{7-\delta}$ and oxygen compositions determined by weight loss (referenced to a starting composition of $YBa_2Cu_3O_{6.93}$) and iodometric titration. All samples were annealed at 520 °C (except as noted in the footnotes). Estimated errors for the oxygen compositions are 0.01. Samples marked with an asterisk (*) were studied by neutron powder diffraction.

Annealing conditions		Oxygen composition $(7-\delta)$	
$p(O_2)$ (atm)	Time (h)	Weight loss	Titration
*1.00	a	6.93	6.92
1.00	21	6.84	
0.515	25	6.82	
0.30	75	6.78	6.78
*0.12	22	6.73	
0.063	45	6.69	
0.043	48	6.67	
0.029	27	6.64	
*0.019	23	6.60	6.60
0.010	21	6.57	
*0.0095	66	6.55	
0.0050	22	6.52	
0.030	96	6.48	
*0.0027	21	6.48	
*0.001 75	22	6.45	
*0.001 07	21	6.40	6.39
0.001 00	22	6.40	
*0.000 700	47	6.38	
*0.000 415	23	6.34	
*0.000 195	66	6.28	6.29
*0.000 100	b	6.09	

[a]Cooled slowly from 960 °C in flowing oxygen as described in the text.

[b]Annealed at 640 °C for 47 h, then cooled to 520 °C and quenched into liquid nitrogen as described in text.

gen pressure indicator at the output of the furnace. The annealing time was varied from 24 h for the high-oxygen-content samples to 96 h for the low-oxygen-content samples. Following the anneals, the samples were quenched from 520 °C into liquid nitrogen. The oxygen stoichiometries of the quenched samples made by this technique were varied from 6.84 to 6.28 by controlling the oxygen partial pressure in the range of 1 to 2×10^{-4} atm. The annealing conditions for each sample are listed in Table I. In order to extend the range of oxygen stoichiometry in our study, an additional sample with an oxygen content of 6.09 was made by annealing for 47 h in nitrogen gas containing 100 ppm oxygen at 640 °C, then cooling at 120 °C/h to 520 °C, followed by a quench into liquid nitrogen. The oxygen stoichiometries of the samples were determined by measuring weight changes induced by the heat treatment process, by Rietveld refinement of neutron-diffraction data, and, for some samples (see Table I), by iodometric titration.

Weight changes were monitored on small bars weighing 0.1–0.2 g. The bars were dry cut with a diamond saw, lightly sanded, buffed to remove all loose powder, and dried with a hair blower (being careful that sample temperatures did not exceed 100 °C). One or more bars were weighed and then included with each sample during the high-temperature anneal. After the quench, these small bars were warmed to room temperature, blown dry, and weighed with a Mettler microgram balance to determine the weight loss during the anneal-quench process from which the oxygen composition of the sample was calculated.

In addition to the weight-loss measurements, which were performed for every sample, oxygen compositions were determined by iodometric titration[33,34] for five samples. Table I compares the compositions determined by weight loss and iodometric titration. The largest differences between weight-loss and iodometric titration measurements are on the order of 0.01. Since the master batch was found to exhibit variations in oxygen composition of the same magnitude, the largest absolute error in oxygen composition for a sample determined solely by weight-loss measurements could be as large as 0.02.

Figure 2 shows oxygen compositions as determined from weight-loss measurements and iodometric titration plotted versus the oxygen partial pressure in which the samples were equilibrated at 520 °C before quenching into liquid nitrogen. The weight-loss measurements are referenced to a starting composition of $YBa_2Cu_3O_{6.93}$. Other published work shows similar results for *in situ* measurements of composition versus temperature and oxygen partial pressure, indicating that the composition does not change significantly during the quench.[35–40]

Meissner effect measurements in fields <10 G were performed on all samples to determine the bulk superconducting transition temperatures. The measurements were done on warming after initially cooling the samples in the measuring field to 4.2 K. On selected samples the shielding and flux trapping were also measured. T_c's were also determined by measuring resistively with a four-probe ac technique at 100 Hz using 1.5-mA measuring current in zero field from 4.2 to 300 K in a gas flow cryostat. Complete details of these measurements will be reported in a separate paper.[41]

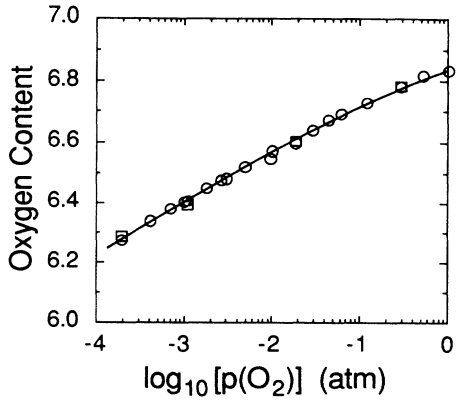

FIG. 2. Oxygen compositions for samples of $YBa_2Cu_3O_{7-\delta}$ determined by weight-loss measurements, referenced to a starting composition of $YBa_2Cu_3O_{6.93}$ (open circles), and by iodometric titration (open squares) vs the oxygen partial pressure at which the samples were equilibrated at 520 °C before quenching into liquid nitrogen.

The bulk superconducting transition temperatures determined from the Meissner effect measurements as a function of oxygen composition are shown in Fig. 3. T_c's determined from resistivity measurements ($\rho=0$) yield a similar result. Clear two-plateau behavior is observed. The error bars extend from the Meissner onset temperature to the temperature at which 50% of the total Meissner effect is observed. It is clear from these data that in

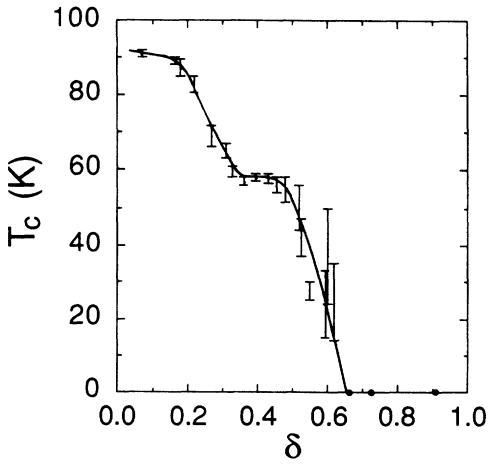

FIG. 3. Superconducting transition temperatures, T_c, for oxygen-deficient samples of $YBa_2Cu_3O_{7-\delta}$, produced by quenching into liquid nitrogen from various oxygen partial pressures at 520 °C. The error bars for T_c extend from the Meissner onset temperature to the temperature at which the Meissner signal is 50% of its maximum value. The oxygen compositions, δ, are determined from weight-loss measurements referenced to a starting composition of $YBa_2Cu_3O_{6.93}$ (see text).

the range $0<\delta<0.2$, which is commonly referred to as the 90-K plateau, T_c is not actually constant, but decreases by a small, but real, amount. However, T_c does appear to be constant with a value near 56 K for $0.35<\delta<0.45$, within the accuracy of our measurements. For $\delta>0.5$, T_c drops rapidly, reaching zero near $\delta=0.65$. In this range of compositions, the superconducting transitions become broad, making a more accu-

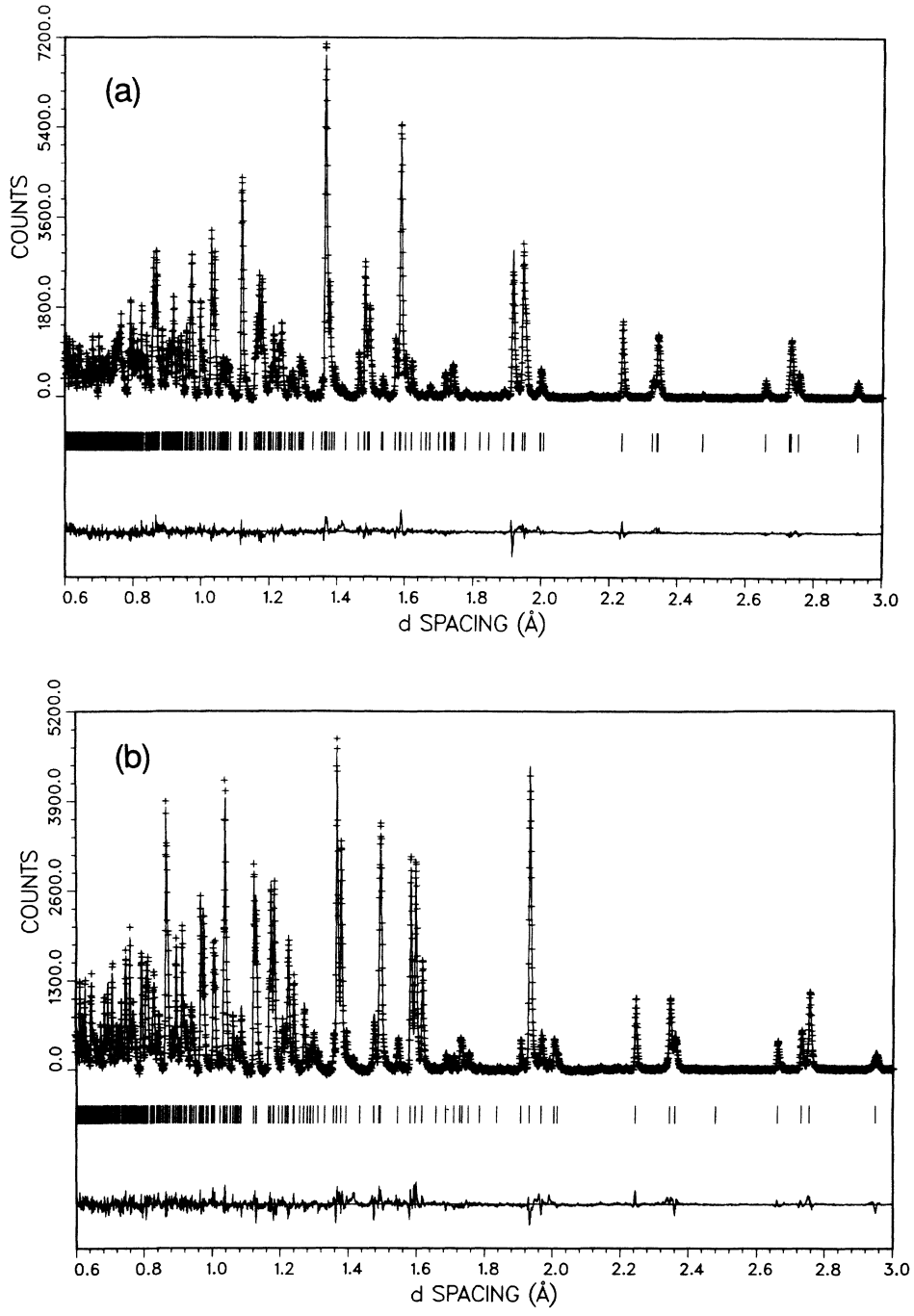

FIG. 4. Rietveld refinement profiles for (a) orthorhombic (space group *Pmmm*) $YBa_2Cu_3O_{6.73}$ and (b) tetragonal (space group *P4/mmm*) $YBa_2Cu_3O_{6.28}$. The plus signs (+) are the raw time-of-flight neutron powder diffraction data. The solid line is the calculated profile. Tick marks below the diffraction profile mark the positions of allowed Bragg reflections. The background was fit as part of the refinement but has been subtracted prior to plotting. A difference curve (observed minus calculated) is plotted at the bottom.

rate determination of the point at which T_c reaches zero difficult. Such behavior may result from sample inhomogeneity, which becomes more severe at lower oxygen concentrations for samples made by this technique. Since the intrinsic T_c is dropping very rapidly in this composition range, a small amount of inhomogeneity would result in substantial broadening of the measured superconducting transition.

NEUTRON POWDER DIFFRACTION MEASUREMENTS

Eleven of the samples were made in large enough quantities (>4 g) for neutron powder diffraction measurements. The neutron powder diffraction data were collected at room temperature for samples weighing 4–8 g by the time-of-flight technique using the Special Environment Powder Diffractometer at the Intense Pulsed Neutron Source[42] (IPNS). Typical data collection times were 4 h per sample. The data were analyzed in either the orthorhombic *Pmmm* or tetragonal *P4/mmm* space groups by the Rietveld structure refinement technique[43] to obtain structural parameters, including oxygen site occupancies for the different oxygen sites. A typical refinement included approximately 800 orthorhombic or 450 tetragonal reflections covering the range of d spacings from 0.52 to 2.8 Å. Rietveld refinement profiles for orthorhombic $YBa_2Cu_3O_{6.73}$ and tetragonal $YBa_2Cu_3O_{6.28}$ are shown in Fig. 4.

The structural parameters as determined by Rietveld refinement are summarized in Table II. The atoms are identified as shown in Fig. 1. The a and b lattice parameters are plotted in Fig. 5 versus the oxygen content δ. Within the accuracy of our measurements, the orthorhombic-to-tetragonal (O-T) phase transition corresponds to the composition at which superconductivity disappears ($\delta=0.65$). This conclusion is somewhat weakened by the fact that the superconducting transitions become rather broad as T_c approaches zero. However, in the region of the O-T transition, the nearest orthorhombic sample ($\delta=0.62$) is superconducting, while the nearest tetragonal sample ($\delta=0.66$) shows no bulk superconductivity.

The c-axis lattice parameter and unit-cell volume versus δ are shown in Figs. 6 and 7. The observed behavior of the lattice parameters and cell volume is qualitatively consistent with our previous data obtained *in situ* at high temperature in controlled oxygen atmospheres[27,44] and with our previous data for metastable samples prepared by quenching from various temperatures at 1-atm oxygen partial pressure.[16] We see a smooth variation of the lattice parameters, with the or-

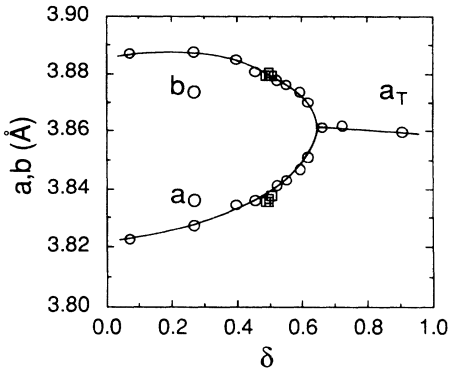

FIG. 5. Lattice parameters, a_O and b_O in the orthorhombic phase and a_T in the tetragonal phase of $YBa_2Cu_3O_{7-\delta}$, determined by Rietveld refinement of neutron powder diffraction data, vs δ. The oxygen compositions, δ, are determined from weight-loss measurements. The open circles are for a consistent set of samples quenched from various controlled oxygen partial pressures at 520°C into liquid nitrogen (Table II). The open squares are for four additional samples made by various quenching and sealed-quartz-tube annealing techniques in order to further investigate the behavior near $\delta=0.05$ (Table III, see text). Error bars, taken as the statistical standard deviations from the Rietveld refinement, are smaller than the symbols.

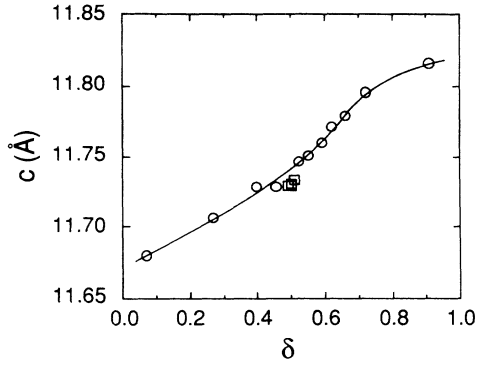

FIG. 6. c-axis lattice parameter vs δ for $YBa_2Cu_3O_{7-\delta}$. Format is the same as for Fig. 5. Error bars are smaller than the symbols.

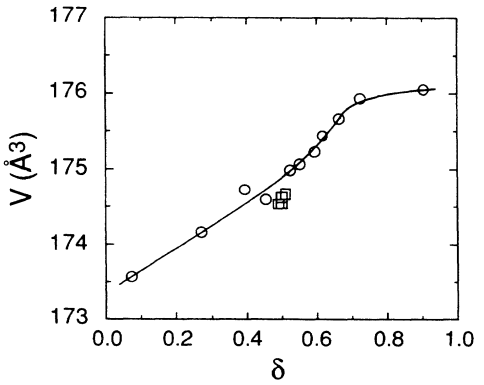

FIG. 7. Unit-cell volume, V, vs δ for $YBa_2Cu_3O_{7-\delta}$. Format is the same as for Fig. 5. Error bars are smaller than the symbols.

TABLE II. Structural parameters for oxygen-deficient samples of $YBa_2Cu_3O_{7-\delta}$, annealed in controlled oxygen atmospheres at 520 °C and then quenched into liquid nitrogen. Rietveld refinements were done in the orthorhombic *Pmmm* or tetragonal *P4/mmm* space groups. Atom positions are Y($\frac{1}{2},\frac{1}{2},\frac{1}{2}$), Ba($\frac{1}{2},\frac{1}{2},z$), Cu(1)(0,0,0), Cu(2)(0,0,z), O(1)(0,$\frac{1}{2}$,0), O(2)($\frac{1}{2}$,0,z), O(3)(0,$\frac{1}{2}$,z), O(4)(0,0,z), and O(5)($\frac{1}{2}$,0,0). Numbers in parentheses are statistical standard deviations of the last significant digit.

δ (weight loss)		0.07[a]	0.27	0.40	0.45
	a (Å)	3.8227(1)	3.8275(1)	3.8349(1)	3.8362(1)
	b (Å)	3.8872(2)	3.8875(1)	3.8851(1)	3.8808(1)
	c (Å)	11.6802(2)	11.7063(2)	11.7279(2)	11.7286(2)
	V (Å^3)	173.56	174.18	174.73	174.61
Y:	B (Å^2)	0.28(3)	0.33(3)	0.24(4)	0.36(3)
Ba:	z	0.1843(2)	0.1871(2)	0.1879(2)	0.1892(2)
	B (Å^2)	0.44(3)	0.48(3)	0.40(4)	0.44(4)
Cu(1):	B (Å^2)	0.41(3)	0.53(3)	0.61(4)	0.63(4)
Cu(2):	z	0.3556(1)	0.3569(1)	0.3578(1)	0.3579(1)
	B (Å^2)	0.20(2)	0.24(2)	0.18(3)	0.21(2)
O(1):	U^2_{11} (Å^2)	0.022(3)	0.031(3)	0.033(5)	0.036(5)
	U^2_{22} (Å^2)	−0.001(2)	0.006(2)	0.012(3)	0.002(3)
	U^2_{33} (Å^2)	0.019(2)	0.013(3)	0.016(4)	0.023(5)
	n	0.90(1)	0.74(1)	0.69(2)	0.56(1)
O(2):	z	0.3779(2)	0.3788(2)	0.3786(2)	0.3787(2)
	B (Å^2)	0.51(4)	0.46(4)	0.45(5)	0.47(4)
O(3):	z	0.3790(2)	0.3780(2)	0.3779(2)	0.3784(2)
	B (Å^2)	0.35(3)	0.28(3)	0.07(4)	0.34(4)
O(4):	z	0.1590(2)	0.1572(2)	0.1561(2)	0.1559(2)
	U^2_{11} (Å^2)	0.009(1)	0.015(1)	0.016(2)	0.011(1)
	U^2_{22} (Å^2)	0.007(1)	0.18(1)	0.018(2)	0.015(1)
	U^2_{33} (Å^2)	0.010(1)	0.003(1)	−0.005(1)	0.009(1)
	n	2.06(2)	2.03(2)	1.94(2)	2.00(2)
O(5):	n	0.03(1)	0.03(1)	0.04(1)	0.04(1)
	Peak width	8.1(1)	7.3(1)	7.5(1)	7.3(1)
	R_{wp} (%)	5.96	5.69	6.74	5.98
	R_{expt} (%)	3.33	3.64	3.77	3.65

δ (weight loss)		0.52	0.55	0.59	0.62
	a (Å)	3.8415(1)	3.8433(1)	3.8468(1)	3.8510(1)
	b (Å)	3.8778(1)	3.8764(1)	3.8736(1)	3.8700(1)
	c (Å)	11.7470(2)	11.7512(2)	11.7601(2)	11.7711(2)
	V (Å)	174.99	175.07	175.24	175.43
Y:	B (Å^2)	0.23(4)	0.40(4)	0.27(4)	0.38(4)
Ba:	z	0.1896(2)	0.1904(2)	0.1905(2)	0.1915(2)
	B (Å^2)	0.49(5)	0.48(4)	0.49(5)	0.58(5)
Cu(1):	B (Å^2)	0.74(5)	0.79(4)	0.74(4)	0.81(4)
Cu(2):	z	0.3587(2)	0.3588(1)	0.3592(1)	0.3596(1)
	B (Å^2)	0.26(3)	0.23(3)	0.22(3)	0.27(3)
O(1):	U^2_{11} (Å^2)	0.033(6)	0.036(7)	0.028(7)	0.038(9)
	U^2_{22} (Å^2)	0.018(5)	−0.001(4)	0.013(5)	−0.009(5)
	U^2_{33} (Å^2)	0.015(6)	0.047(8)	0.050(9)	0.097(15)
	n	0.56(2)	0.45(2)	0.48(2)	0.38(2)
O(2):	z	0.3787(3)	0.3785(3)	0.3791(3)	0.3794(4)
	B (Å^2)	0.40(5)	0.50(4)	0.39(5)	0.42(6)
O(3):	z	0.3778(3)	0.3787(3)	0.3779(3)	0.3778(4)

TABLE II. (*Continued.*)

δ (weight loss)		0.52	0.55	0.59	0.62
	B (Å^2)	0.20(5)	0.35(4)	0.29(5)	0.48(6)
O(4):	z	0.1553(2)	0.1547(2)	0.1543(2)	0.1536(2)
	U_{11}^2 (Å^2)	0.021(2)	0.014(2)	0.020(2)	0.016(2)
	U_{22}^2 (Å^2)	0.022(2)	0.016(2)	0.019(2)	0.018(2)
	U_{33}^2 (Å^2)	−0.009(1)	0.010(1)	−0.005(1)	0.002(1)
	n	1.96(2)	2.00(2)	1.95(2)	1.96(2)
O(5):	n	0.06(1)	0.04(1)	0.08(1)	0.12(2)
Peak width		7.3(1)	6.9(1)	7.1(1)	7.1(1)
R_{wp} (%)		8.21	6.24	6.77	6.43
R_{expt} (%)		3.71	3.88	3.71	4.20

δ (weight loss)		0.66	0.72	0.91[b]
a (Å)		3.8617(1)	3.8621(1)	3.8600(1)
b (Å)		=a	=a	=a
c (Å)		11.7799(2)	11.7961(2)	11.8168(2)
V (Å^3)		175.67	175.95	176.07
Y:	B (Å^2)	0.51(4)	0.50(3)	0.42(3)
Ba:	z	0.1929(2)	0.1935(2)	0.1946(2)
	B (Å^2)	0.54(5)	0.54(4)	0.50(3)
Cu(1):	B (Å^2)	0.85(5)	0.86(4)	0.91(4)
Cu(2):	z	0.3600(2)	0.3607(1)	0.3611(1)
	B (Å^2)	0.37(3)	0.31(2)	0.37(2)
O(1):	U_{11}^2 (Å^2)	0.052(16)	0.067(14)	$B=2$[c]
	U_{22}^2 (Å^2)	−0.011(6)	−0.004(16)	
	U_{33}^2 (Å^2)	0.056(19)	0.099(19)	
	n	0.32(3)	0.39(2)	0.10(1)
O(2):	z	0.3790(1)	0.3789(1)	0.3795(1)
	B (Å^2)	0.64(3)	0.53(3)	0.62(2)
O(3):	z			
	B (Å^2)			
O(4)	z	0.1529(3)	0.1527(2)	0.1524(2)
	U_{11}^2 (Å^2)	0.012(1)	0.013(1)	0.009(1)
	U_{22}^2 (Å^2)	$=U_{11}^2$	$=U_{11}^2$	$=U_{11}^2$
	U_{33}^2 (Å^2)	0.031(2)	0.007(1)	0.031(2)
	n	2.01(2)	1.87(2)	2.00(2)
O(5):	n			
Peak width		8.9(1)	7.2(1)	7.0(1)
R_{wp} (%)		8.15	7.30	7.97
R_{expt} (%)		3.93	3.95	3.55

[a]Slowly cooled in 1 atm of oxygen.
[b]Annealing schedule differs from other samples as described in the text.
[c]At this low occupancy, B(O(1)) cannot be refined. It is fixed at $B(O(1))=2$ Å^2.

thorhombic strain (b-a) decreasing to zero at an oxygen content of 6.35, where the orthorhombic structure collapses into tetragonal symmetry. The c lattice parameter increases smoothly as oxygen is removed, showing no measurable discontinuity at the *O-T* phase transition. As observed previously in *in situ* measurements,[44] the variation of the c axis versus x is somewhat larger in the orthorhombic phase near the *O-T* transition because of the rapid variation of oxygen site occupancies in this composition range. However, we observe no discontinuous variation of the c axis in this range as was recently reported for samples prepared at 415 °C by zirconium gettering.[4]

Remarkably, the cell volume (Fig. 7) increases as oxygen is removed. The total increase is about 1% and is

mainly because of the expansion of the unit cell along the *c* direction. There is no discontinuity in the cell volume at the *O-T* phase transition, consistent with a transition of second order. However, the cell volume does exhibit a different dependence on δ in the orthorhombic and tetragonal phases.

We find the *O-T* phase transition to occur at a lower oxygen stoichiometry ($\delta=0.65$) than reported for our samples quenched from higher temperatures[16] or examined by *in situ* neutron diffraction.[44] The discrepancy with our first *in situ* neutron-diffraction experiment apparently results from the occurrence of additional oxygen vacancies on the O(4) site, which were overlooked in the original structure refinements.[27,45] Several other authors have also reported observing the *O-T* transition at a total oxygen concentration near 6.4 for oxygen-deficient metastable samples produced by various techniques.[4–6] Except for some of the earliest work, where the problems of sample inhomogeneity resulting from insufficient oxygen annealing were not fully appreciated, we believe that departures from a value near 6.4 result mostly from the method used to determine δ rather than from real differences in the samples. The most prevalent error may be the incorrect assumption that a fully oxygenated sample has an oxygen content of exactly 7.00. However, at least one author has reported the synthesis of orthorhombic $YBa_2Cu_3O_{7-\delta}$, with a total oxygen concentration near 6.3 as measured by hydrogen reduction.[3] Thus, the possibility that specific annealing techniques may alter the composition at which the *O-T* transition occurs cannot be ruled out. Moreover, *in situ* studies (e.g., TGA and resistivity measurements) suggest that the oxygen stoichiometry at the *O-T* transition may be a function of temperature and oxygen partial pressure, tending toward lower oxygen content at lower temperatures and oxygen partial pressures. However, existing experimental data are sufficiently divergent to preclude firm conclusions about the phase diagram over a wide range of temperatures and partial pressures.[46–48]

The homogeneity of the samples can be assessed from the quality of the Rietveld structure refinements. The Bragg peaks are observed to broaden somewhat with decreasing oxygen concentration, especially in the orthorhombic phase near the orthorhombic-to-tetragonal transition, and then become sharper again upon entering the tetragonal phase. The observed broadening is anisotropic and asymmetric. One possible explanation for this behavior is that the oxygen content is inhomogeneous in each sample, leading to peak broadening, which is largest in the range of δ, where the lattice parameters vary most sharply with δ. Since (with increasing δ) the *b*-axis lattice constant decreases, while those for *a* and *c* increase, in the region close to the transition, the asymmetry of the peak broadening is also explained by such a model. Assuming that this explanation is correct, we have estimated that the oxygen inhomogeneity (in the worst case for large values of δ) has an upper limit $\Delta\delta=0.1$.

A second explanation for the observed broadening is that the sample is separated into two phases with different oxygen contents. If the two phases were to have significantly different oxygen stoichiometries, however, this two-phase behavior should be apparent in our Fig. 2. The oxygen partial pressure should remain constant across the two-phase region. Thus, we must conclude that phase separation does not occur at the temperatures at which our samples are equilibrated. However, it is not impossible that phase separation does occur at a lower temperature, and that it occurs in our samples upon cooling. In this context, it is important to note that recent thermodynamic measurements of Tetenbaum *et al.* show what these authors interpret as indirect evidence for a miscibility gap below a critical temperature of about 215 °C and centered at a composition of $\delta=0.35$.[49] Additionally, a recent electron-diffraction study versus δ by Beyers *et al.* shows two-phase samples only at oxygen contents where plateaus in T_c occur, suggesting that the plateaus result from phase separation.[50] If such an explanation is correct, it is not surprising that the phase separation is poorly developed in our samples, since the rapid cooling inside the miscibility gap could prevent the long-range diffusion that would be required to achieve complete phase separation.

Rietveld refinements were attempted in which the model included two orthorhombic phases of differing oxygen stoichiometry or a model based on a mixture of an orthorhombic and a tetragonal phase. Neither model was stable enough to give a suitable refinement of the data. However, correlations are unavoidably high for such a model because the differences in lattice parameters are small compared to the instrumental resolution, and these attempts should not be taken as evidence that phase separation does not occur. In particular, it is possible that the refinement is hindered by intrinsic peak broadening because the phase separation is not well developed over long ranges, as discussed earlier.

The site occupancies of each of the five oxygen sites (Fig. 8) have been obtained from Rietveld refinement (Table II). The O(2) and O(3) sites are fully occupied and remain so at all oxygen stoichiometries. Thus, these occupancies were constrained at their ideal values in the final refinements. The occupancies of the O(1), O(5), and O(4) sites are shown in Fig. 8. The dominant effect with reduced oxygen content is the continuous removal of oxygen atoms from the O(1) site that forms the one-dimensional Cu-O chains in the fully ordered $YBa_2Cu_3O_7$ structure. The O(1) site occupancy decreases from 0.90(1) for the original $YBa_2Cu_3O_{6.93}$ sample to a value slightly below 0.25 at the *O-T* phase transition. There is a much smaller change in the O(5) occupancy. This occupancy remains near zero for $\delta<0.5$ and then rises rapidly to meet the O(1) occupancy at the *O-T* phase transition.

In our previous data for samples quenched from a high temperature into liquid nitrogen and for *in situ* neutron-diffraction experiments, we have seen evidence for vacancies on the O(4) oxygen site.[16,27,44,45,51] Unfortunately, the standard deviations are often high, apparently because this variable appears to be highly correlated to possible sources of systematic error such as preferred orientation and line broadening. However, a comparison of the total oxygen content determined by neutron diffraction with that determined by other methods sup-

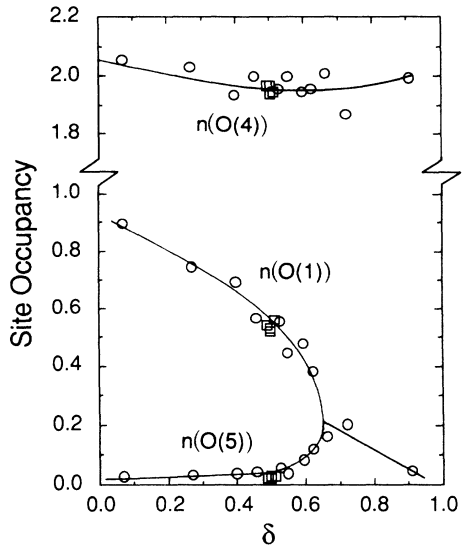

FIG. 8. Oxygen site occupancies for the O(1), O(4), and O(5) sites in $YBa_2Cu_3O_{7-\delta}$ (see Fig. 1 and Tables II and III) vs δ. Format is the same as for Fig. 5. Error bars (statistical standard deviations) are nominally the size of the symbols.

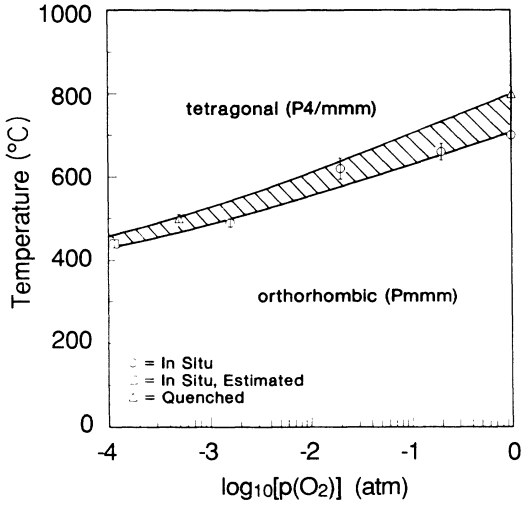

FIG. 9. Temperature of the orthorhombic-to-tetragonal (*O-T*) phase transitions in $YBa_2Cu_3O_{7-\delta}$ vs oxygen partial pressure for samples studied by *in situ* neutron powder diffraction (Refs. 27, 44 and 51) and for samples quenched from the indicated conditions into liquid nitrogen (Ref. 16 and the present work). These results show a systematic offset between the phase boundaries determined by the two techniques. The shaded region is the area of the phase diagram for which *in situ* samples are tetragonal, while quenched samples are orthorhombic.

ports the existence of O(4) vacancies. Thus, the O(4) site occupancy was allowed to vary in the present refinements. The results are shown in Fig. 8. The data suggest an increase in the number of oxygen vacancies with increasing δ, reaching a maximum of 0.05–0.1 near $\delta=0.7$. As expected based on bonding arguments, no O(4) vacancies are present at $\delta=1$. [Since all basal plane oxygen sites are vacant at $\delta=1$, the structure would not be stable without fully occupied O(4) sites.]

When the present data are compared with those obtained from recent *in situ* neutron-diffraction data taken at a constant temperature of 490 °C versus oxygen partial pressure (i.e., conditions which simulate those from which the present samples were quenched),[27,44,51] it is clear that a small region of the temperature–oxygen-partial-pressure phase diagram exists for which orthorhombic samples are produced by quenching from conditions where the *in situ* structure is tetragonal. A summary of our measurements of the *O-T* transition for both kinds of experiments is shown in Fig. 9. The shaded region of this figure is the region of the phase diagram where we observe tetragonal symmetry *in situ* but orthorhombic symmetry for samples quenched into liquid nitrogen. The observed differences are too large to be explained by the bulk diffusion of oxygen into the sample during the quenching process. The most likely explanation for such behavior is that orthorhombic symmetry, resulting from ordered oxygen vacancies, persists to significantly lower total oxygen concentrations at lower temperatures and that the diffusion kinetics for chain ordering (which requires only short-range hopping) is sufficiently rapid that some additional ordering occurs during the liquid-nitrogen "quench." The implication of such a hypothesis is that quenching from 500 °C may not produce homogeneous samples; rather they are frozen in an intermediate state as they attempt to achieve a degree of oxygen vacancy ordering consistent with the lower temperature. This conclusion is consistent with the Bragg peak broadening observed for the present samples and implies that future studies should use samples equilibrated at a lower temperature.

Even though some subtle differences in the degree of chain order may exist between *in situ* and metastable oxygen-deficient samples, the *O-T* transition observed in this experiment appears to be continuous. Plots of either of the two order parameters, i.e., the orthorhombic strain (b-a) or the oxygen chain-site-occupancy order parameter derived from site occupancies [n(O(1))-n(O(5))], as a function of δ both exhibit the behavior expected for a second-order transition, extrapolating smoothly to zero at the *O-T* transition. A more severe test, which avoids the need to assign a critical exponent, is to plot one order parameter versus the other. Such a plot is shown in Fig. 10, where the chain order parameter [n(O(1))-n(O(5))] is plotted as a function of the orthorhombic strain (b-a). Within the uncertainties, the data can be fit with a straight line passing through the origin, as expected for a well-behaved second-order phase transition.

The Cu(1)—O(4) and Cu(2)—O(4) bond lengths versus δ are shown in Fig. 11. Additional published bond-length data, also determined by neutron powder diffraction, have been included in this plot for comparison.[1,52–56] (Note that several other published bond lengths have been omitted either because the oxygen concentration of the sample was not measured by an independent tech-

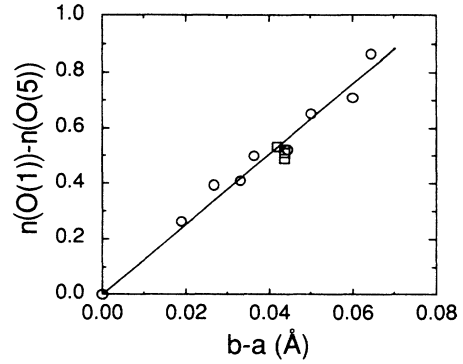

FIG. 10. Oxygen chain-site-occupancy order parameter $[n(O(1))-n(O(5))]$ vs the orthorhombic strain $(b-a)$ for oxygen-deficient samples of $YBa_2Cu_3O_{7-\delta}$. The data can be fit with a straight line passing through the origin, which is consistent with the *O-T* transition being a well-behaved second-order transition.

nique or because the structural refinement exhibited obvious problems.) Starting from $\delta=0$, within the orthorhombic phase, the Cu(1)—O(4) bond length decreases and the Cu(2)—O(4) bond length increases with increasing δ. Within the uncertainties, the variation is linear for $0<\delta<0.5$. In the tetragonal phase for $0.6<\delta<1.0$, the variation of both bond lengths is also essentially linear,

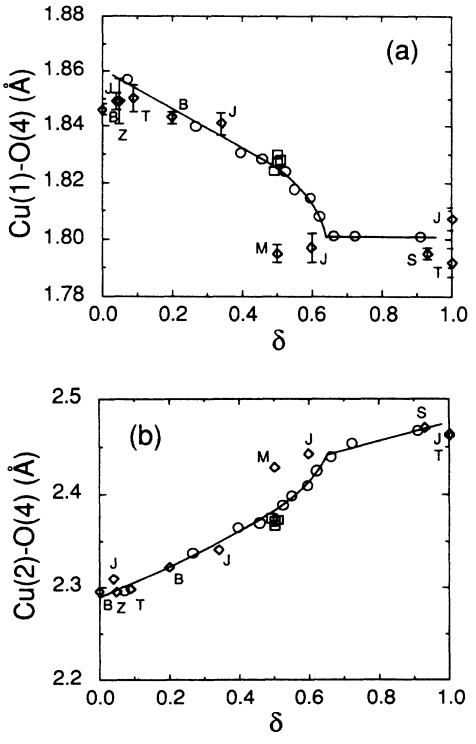

FIG. 11. Copper-oxygen bond lengths (a) Cu(1)—O(4) and (b) Cu(2)—O(4) (in Å) as a function of δ for oxygen-deficient samples of $YBa_2Cu_3O_{7-\delta}$. Format is the same as for Fig. 5. Data marked by open diamonds are taken from the published literature as follows: *J*, Ref. 1; *T*, Ref. 52; *B*, Ref. 55; *M*, Ref. 54; *Z*, Ref. 56; and *S*, Ref. 53. Where no error bars are shown, they are nominally the size of the symbols.

but with much smaller slopes. These two regions are smoothly connected by a small region, $0.5<\delta<0.6$, in which the bond lengths vary rapidly. This region of rapid variation is, of course, the same range of concentrations in which the oxygen site occupancies and lattice constants are changing rapidly as the *O-T* transition is approached and is, thus, not unexpected.

These results are significantly different from those presented by Cava *et al.*, in which it is claimed that an almost discontinuous change in these Cu—O bond lengths occurs at a concentration within the orthorhombic phase.[4] Their conclusion is based on bond lengths for four oxygen concentrations taken from the literature.[53–55] The same four points have been included in Fig. 11 (the points labeled *B* at $\delta=0$, *B* at $\delta=0.2$, *M* at $\delta=0.5$, and *S* at $\delta=0.93$). Three of the points agree well with the present data. However, the point at $\delta=0.5$ (Ref. 54) falls far off the present curve. Based on a careful reading of the original paper by Miraglia *et al.*[54] it is possible to propose some explanations for the discrepancy. Their sample was made by annealing a mixture of equal amounts of $YBa_2Cu_3O_7$ and $YBa_2Cu_3O_6$ at 450 °C for 16 h in a sealed silica tube. An error in the assumed compositions of the starting materials could have resulted in an incorrect assignment of the oxygen concentration. Comparison of the refined lattice constants with the present data suggests an oxygen concentration closer to 6.45. Another error may have resulted from incorrect constraints used in the structural refinement. The oxygen site occupancies were all constrained to their ideal values with O(1) half occupied, O(2), O(3), and O(4) fully occupied, and O(5) empty. (Note that the sites have been identified according to Fig. 1 rather than the scheme used in Ref. 54.) These constraints could have biased the refinement of atom positions, resulting in the incorrect bond length.

In an attempt to further resolve this discrepancy, four additional samples with oxygen concentrations near 6.5 were made (see Table III). One sample was made by quenching into liquid nitrogen, annealing at 500 °C and an oxygen partial pressure of 0.0039 atm, and then a second sample was made by annealing a previously quenched sample (with $\delta\approx0.5$) in an evacuated sealed quartz tube for 2.5 h at 500 °C, followed by 336 h at 300 °C. The third and fourth samples were made simultaneously in an evacuated sealed quartz tube. The sealed tube contained the starting materials $YBa_2Cu_3O_{6.92}$ and $YBa_2Cu_3O_{6.09}$ in physically separated locations in appropriate quantities so that, after annealing for 312 h at 350 °C, both samples were single phase and exhibited the same oxygen concentrations (6.50 ± 0.02), as determined by carefully monitoring the weight changes. The 6.09 sample was made from the same master batch at the 6.92 sample with an intermediate heat treatment and quench. The final sealed-tube stoichiometries were in agreement with the results from neutron powder diffraction. The Cu(1)—O(4) and Cu(2)—O(4) bond lengths determined by Rietveld refinement of neutron powder diffraction data for these four samples were essentially identical to our original result and have been included in Fig. 11 (and all of the other figures of structural parameters) as the

square symbols. Thus, we are not able to duplicate the bond length reported by Miraglia *et al.* for $YBa_2Cu_3O_{6.50}$, and we conclude that it should be considered suspect until it is confirmed. Complete structural data for these additional samples are given in Table III.

It is interesting to consider the cause of the large variation in the Cu(1)—O(4) and Cu(2)—O(4) bond lengths shown in Fig. 11. The simplest explanation is that the Cu—O bond for a Cu ion with two oxygen neighbors is intrinsically much shorter than that for a Cu ion with four oxygen neighbors. As oxygen is removed from the structure, Cu(1) is reduced and its average coordination number changes from 4 for $\delta=0$ to 2 for $\delta=1$. Analysis of diffraction data, of course, gives the spatial average of the individual bond lengths in the sample and would be expected to show a decreasing average bond length with increasing δ. This simple picture is, however, not an adequate explanation for the observed behavior, since the predicted variation with δ would be the same in both the orthorhombic and tetragonal phases if average coordination number were the only consideration. The pronounced change in bond lengths within the orthorhombic phase, where T_c is varying with δ, suggests that significant charge-transfer effects are occurring. It is now generally believed that superconductivity occurs in the two-dimensional CuO_2 planes. Arguably, metallic behavior in the planes results from excess charge holes contributed by the one-dimensional CuO_x chains, i.e., the chains act as insulating reservoirs of charge.[4,30–32] The removal of oxygen can either reduce Cu(1) or remove holes from the conducting planes via a charge-transfer mechanism with accompanying changes in bond lengths.[57–59]

TABLE III. Refined structural parameters for additional oxygen-deficient samples of $YBa_2Cu_3O_{7-\delta}$ made by various quenching and sealed-quartz-tube techniques as discussed in the text. Refinement models are the same as in Table II.

	Sample[a]	A	B	C	D
	δ (weight loss)	0.50	0.50	0.49	0.51
	a (Å)	3.8358(1)	3.8366(1)	3.8358(1)	3.8375(1)
	b (Å)	3.8796(1)	3.8804(1)	3.8797(1)	3.8794(1)
	c (Å)	11.7295(2)	11.7300(2)	11.7293(2)	11.7329(2)
	V (Å)	174.55	174.63	174.55	174.67
Y:	B (Å^2)	0.39(3)	0.39(3)	0.39(3)	0.35(3)
Ba:	z	0.1887(2)	0.1894(2)	0.1889(2)	0.1885(2)
	B (Å^2)	0.54(4)	0.49(4)	0.53(3)	0.52(2)
Cu(1):	B (Å^2)	0.66(4)	0.63(4)	0.64(3)	0.69(4)
Cu(2):	z	0.3578(1)	0.3579(1)	0.3579(1)	0.3580(1)
	B (Å^2)	0.28(2)	0.26(2)	0.28(2)	0.30(3)
O(1):	U_{11}^2 (Å^2)	0.031(5)	0.040(6)	0.034(4)	0.038(9)
	U_{22}^2 (Å^2)	0.002(3)	0.000(3)	0.002(2)	0.005(3)
	U_{33}^2 (Å^2)	0.018(5)	0.020(5)	0.017(4)	0.020(5)
	n	0.53(1)	0.52(2)	0.54(1)	0.56(1)
O(2):	z	0.3789(2)	0.3786(2)	0.3785(2)	0.3787(2)
	B (Å^2)	0.50(4)	0.50(4)	0.48(3)	0.51(4)
O(3):	z	0.3778(2)	0.3780(2)	0.3776(2)	0.3777(2)
	B (Å^2)	0.35(4)	0.38(4)	0.32(3)	0.28(4)
O(4):	z	0.1560(2)	0.1558(2)	0.1555(2)	0.1558(2)
	U_{11}^2 (Å^2)	0.012(1)	0.009(1)	0.013(1)	0.015(1)
	U_{22}^2 (Å^2)	0.012(1)	0.010(1)	0.014(1)	0.014(1)
	U_{33}^2 (Å^2)	0.004(1)	0.009(1)	0.003(1)	−0.002(1)
	n	1.94(2)	1.97(2)	1.97(1)	1.95(2)
O(5):	n	0.02(1)	0.03(1)	0.02(1)	0.03(1)
	Peak width	7.9(1)	8.4(1)	7.3(1)	8.2(1)
	R_{wp} (%)	5.76	6.68	5.25	5.78
	R_{expt} (%)	3.81	4.55	3.25	3.07

[a]A: Quenched into liquid nitrogen after equilibrating at 500 °C in 0.0039 atm of oxygen. B: Quenched as for sample "*A*" and then annealed in a sealed quartz tube for 2.5 h at 500 °C followed by 336 h at 300 °. C: Annealed in a sealed quartz tube for 312 h at 350 °C. ($YBa_2Cu_3O_{6.92}$ initial composition; see text). D: Annealed in a sealed quartz tube for 312 h at 350 °C. ($YBa_2Cu_3O_{6.09}$ initial composition; see text).

As pointed out by Miceli *et al.*,[60] in a charge-transfer model, other structural parameters besides Cu—O bond lengths should also show large variations with oxygen composition. Indeed, the Cu—O bond lengths may not be the most sensitive to charge distribution. For example, the bonding of the Ba atom to the neighboring oxygen atoms, especially O(1)/O(5) in the "chain" layer and O(2)/O(3) in the "plane" layer, would also be expected to change and, in fact, may be associated with a larger net charge transfer than changes in the O(4) position, since O(4) remains strongly bonded to Cu(1) and weakly bonded to Cu(2) at all compositions. The fractional Ba position along the z direction, expressed as the fraction of the distance from the O(1)/O(5) plane ($z=0$) to the average O(2)/O(3) plane [$z=[z(\mathrm{O}(2))+z(\mathrm{O}(3))]/2$], versus δ is plotted in Fig. 12. The variation from 0.487 to 0.513 corresponds to an effective displacement of over 0.3 Å, which is significantly larger than that observed for either Cu—O bond length (Fig. 11).

Large changes in atom-atom distances are not confined to the region linking the "plane" and "chain" layers of the structure. Another direct structural probe of the amount of charge in the CuO_2 planes is the Cu(2)—Cu(2) distance along the z direction. The Cu(2)—Cu(2) separation is plotted as a function of δ in Fig. 13. This distance changes by almost 0.1 Å upon going from 90-K superconducting to insulating behavior. As for the other structural parameters, the variation is relatively smooth within each phase, with a change in slope near the *O-T* transition. However, the data point at $\delta=0.66$ appears to fall on the orthorhombic curve rather than the tetragonal curve. Since this sample falls almost directly on the *O-T* transition, it is not impossible that it is mixed phase, leading to a systematic error in the refinement.

Clearly, various structural parameters that vary with δ can be correlated to T_c in the $YBa_2Cu_3O_{7-\delta}$ system. Some authors have attempted to establish similar correlations for chemically substituted systems. Miceli *et al.*, for example, have postulated that T_c is a simple function

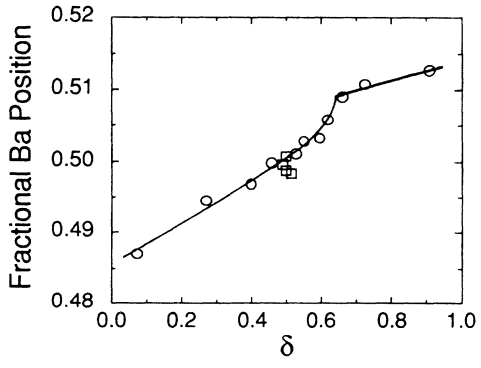

FIG. 12. Fractional Ba atom position in $YBa_2Cu_3O_{7-\delta}$, expressed as a fraction of the distance from the O(1)/O(5) plane ($z=0$) to the average O(2)/O(3) plane [$z=[z(\mathrm{O}(2))+z(\mathrm{O}(3))]/2$], vs δ. Format is the same as for Fig. 5. Error bars are nominally the size of the symbols.

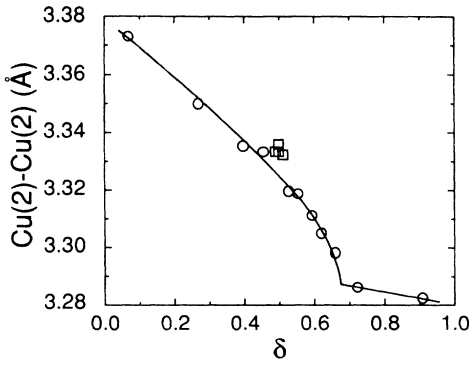

FIG. 13. Cu(2)-Cu(2) distance along the z direction vs δ for $YBa_2Cu_3O_{7-\delta}$. Format is the same as for Fig. 5. Error bars are nominally the size of the symbols.

of the Cu(1)—O(4) bond length for oxygen-deficient and Co-doped [on the Cu(1) site] $YBa_2Cu_3O_{7-\delta}$.[31] Such a proposal leads directly to the idea of a critical Cu(1)—O(4) bond length for superconducting behavior. However, at this point the number of systems for which sufficient data have been reported is too small to argue that the Cu(1)—O(4) length is, indeed, a universal parameter. In fact, data for $Nd_{1+x}Ba_{2-x}Cu_3O_{7+\delta}$ suggest that Cu—O bond lengths are not systematically correlated to T_c, and, thus, are not suitable probes of charge transfer in that system.[61] Concluding whether some of the other structural parameters, e.g., the fractional Ba position or the Cu(2)—Cu(2) distance, are systematically related to T_c must await the publication of data for a wide range of compounds in the $YBa_2Cu_3O_{7-\delta}$ system, doped on the various metal sites and with varied oxygen compositions.

In addition to the atom-atom distances discussed here, T_c can also be correlated with the degree of orthorhombicity or oxygen chain order. For the oxygen-deficient $YBa_2Cu_3O_{7-\delta}$ system, such a hypothesis is immediately suggested by the observation that superconductivity disappears at the *O-T* transition. A plot of T_c versus the oxygen chain order parameter, $n(\mathrm{O}(1))$-$n(\mathrm{O}(5))$, is shown in Fig. 14. Although the correlation between superconductivity and the degree of chain order is quite clear in the oxygen-deficient $YBa_3Cu_3O_{7-\delta}$ compound, the behavior of a number of analogous "1:2:3" compounds, with chemical substitutions on the Y, Ba, or Cu sites, has been used to argue that there is no correlation between cell symmetry and superconductivity. In many compounds of the type $Y_{1-x}M_xBa_2Cu_3O_{7-\delta}$, $YBa_{2-x}M_xCu_3O_{7-\delta}$, and $YBa_2Cu_{3-x}M_xO_{7-\delta}$ increased doping, M, leads to a transition to average tetragonal symmetry, but superconductivity, often with a reduced T_c, persists into the tetragonal phase.[57,59–66] The immediate conclusion of most authors has been that no correlation exists between symmetry and superconductivity. However, more detailed studies have suggested that although the average symmetry of these systems may be tetragonal, the local symmetry is orthorhombic, i.e., ordered Cu-O "chains" exist on a local site. For example, in the case of

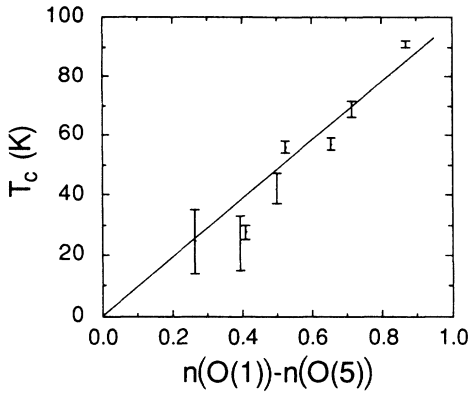

FIG. 14. Superconducting transition temperature, T_c, vs oxygen chain order parameter, n(O(1))-n(O(5)), for $YBa_2Cu_3O_{7-\delta}$. The T_c's are defined as in Fig. 3.

$YBa_2Cu_{3-x}Fe_xO_{7-\delta}$, electron microscopy studies have shown that the superconducting "tetragonal" phase actually consists of small orthorhombic domains in different orientations.[67,68] Even though the degree of chain ordering within these domains may be high, the domains are too small, with respect to the diffraction coherence length, to yield an orthorhombic diffraction pattern.[69] Thus, average tetragonal symmetry is observed.

Additional evidence for such behavior comes from a neutron-diffraction study of $La_{1+x}Ba_{2-x}Cu_3O_{7-\delta}$ versus x in which an attempt was made to determine the degree of oxygen chain order by refining data for the average tetragonal structure with an orthorhombic model.[70] Amazingly, the orthorhombic refinements were stable, even though the orthorhombic strain with near zero, and yielded a chain order parameter, n(O(1))-n(O(5)), which was systematically correlated to T_c. Unfortunately, no other studies in which an attempt has been made to quantify the degree of chain order in systems with average tetragonal structures have been reported. We would propose, however, that the question of whether chain order (or local orthorhombic symmetry) is correlated to superconductivity should remain open until more effort is made to investigate the *local* structures.

CONCLUSIONS

Two overall conclusions can be drawn from this work. First, the observed structural variations as a function of δ are consistent with a "charge-transfer" model in which T_c decreases as carriers (holes) are removed from the two-dimensional CuO_2 planes by the formation of oxygen vacancies in the chains. For the $YBa_2Cu_3O_{7-\delta}$ system, several of the associated bond lengths [i.e., Cu(1)—O(4), Cu(2)—O(4), Cu(2)—Cu(2), etc.] are suitable probes of changes in the local charge distribution. However, without studying other systems it is not possible to conclude whether these probes are applicable in all cases. Indeed, it appears that the degree of chain ordering, if viewed on a local scale, may be the most universally correlated to T_c.

The second conclusion to be drawn is that our neutron powder diffraction data offer no clear explanation for the plateau behavior of T_c at 60 K. In particular, our data do not provide a clear confirmation of either of the two proposals that should be possible to check by diffraction measurements.

Cava *et al.* have proposed that the 60-K plateau is characteristic of a separate phase of $YBa_2Cu_3O_{7-\delta}$, which has a supercell structure because of oxygen vacancy ordering.[3,4,72] Our neutron powder diffraction data show no supercell peaks, suggesting either that the degree of ordering is too weak to be observed or that ordered domains occupy only a small percentage of the sample. Repeated observations using electron[50,71–74] and x-ray diffraction[75] leave no doubt that the supercells exist. However, electron diffraction[72] shows that the ordering is often only two-dimensional, and dark-field electron microscope images[76] show that (when present) domains ordered in three directions can be very small and may occupy only a small fraction of the sample, perhaps explaining our failure to observe supercells by neutron diffraction.

The second explanation previously proposed for the 60-K plateau is that phase separation leads to two-phase samples, one of which has $T_c = 60$ K, over this region of oxygen concentrations.[50] Our neutron powder diffraction data show no conclusive evidence for phase separation. However, we do see line broadening, which is consistent either with phase separation or oxygen inhomogeneity. If the phase-separated regions occur as small (< 100 Å) domains of the supercell phase embedded in a matrix of the 60-K "normal" orthorhombic phase, as seen in the dark-field images,[76] the line broadening we observe (rather than a clear two-phase pattern) is qualitatively what one would expect. Thus, we conclude that our data can be interpreted as being consistent with either model.

ACKNOWLEDGMENTS

The authors wish to acknowledge useful discussions with D. G. Hinks. This work is supported by the U.S. Department of Energy, Basic Energy Sciences–Materials Sciences, under Contract No. W-31-109-ENG-38.

*Permanent address: Department of Physics, University of Illinois at Chicago, Chicago, IL 60680.

†Joint appointment with Department of Physics, Purdue University, West Lafayette, IN 47907.

[1] D. C. Johnston, A. J. Jacobson, J. M. Newsam, J. T. Lewandowski, D. P. Goshorn, D. Xie, and W. B. Yelon, in *Chemistry of High-Temperature Superconductors,* ACS Symposium Series 35, edited by D. L. Nelson, M. S. Whittingham, and T. F. George (American Chemical Society, Washington, D.C., 1987), p. 136; A. J. Jacobson, J. M. Newsam, D. C. Johnson, D. P. Goshorn, J. T. Lewandowski, and M. S. Alvarez, Phys. Rev. B **39**, 254 (1989).

[2]Y. Ueda and K. Kosuge, Physica **156C**, 281 (1988).
[3]R. J. Cava, B. Batlogg, C. H. Chen, E. A. Rietman, S. M. Zahurak, and D. Werder, Phys. Rev. B **36**, 5719 (1987); Nature **329**, 423 (1987).
[4]R. J. Cava *et al.*, Physica **153-155C**, 560 (1988); R. J. Cava, B. Batlogg, K. M. Rabe, E. A. Rietman, P. K. Gallagher, and L. W. Rupp, Jr., *ibid.* **156C**, 523 (1988).
[5]J. M. Tarascon, P. Barboux, B. G. Bagley, L. H. Greene, W. R. McKinnon, and G. W. Hull, in *Chemistry of High-Temperature Superconductors,* ACS Symposium Series, edited by D. L. Nelson, M. S. Whittingham, and T. F. George (American Chemical Society, Washington, D.C., 1987), p. 198.
[6]J. M. Tarascon, L. H. Greene, B. G. Bagley, W. R. McKinnon, P. Barboux, and G. W. Hull, in *Novel Superconductivity,* edited by S. A. Wolf and V. Z. Kresin (Plenum, New York, 1987), p. 705.
[7]P. Meuffels, B. Rupp, and E. Porschke, Physica **156C**, 441 (1988).
[8]B. G. Bagley, L. H. Greene, J.-M. Tarascon, and G. W. Hull, Appl. Phys. Lett. **51**, 622 (1987).
[9]Donglu Shi and D. W. Capone II, Appl. Phys. Lett. **53**, 159 (1988).
[10]E. Takayama-Muromachi, Y. Uchida, M. Ishii, T. Tanaka, and K. Kato, Jpn. J. Appl. Phys. **26**, L1156 (1987).
[11]H. Ihara, H. Oyanagi, S. Sugise, E. Ohno, T. Matsubara, S. Ohashi, N. Terada, M. Jo, M. Hirabayashi, K. Murata, A. Negishi, Y. Kimura, E. Akiba, H. Hayakawa, and S. Shin, Physica **153-155C**, 948 (1988).
[12]M. Tokumoto, H. Ihara, T. Matsubara, M. Hirabayashi, N. Terada, H. Oyanagi, K. Murata, and Y. Kimura, Jpn. J. Appl. Phys. **26**, L1565 (1987).
[13]W. E. Farneth, R. K. Bordia, E. M. McCarron III, M. K. Crawford, and R. B. Flippen, Solid State Commun. **66**, 953 (1988).
[14]W. Wong-Ng, L. P. Cook, C. K. Chiang, L. J. Swartzendruber, L. H. Bennett, J. Blendell, and D. Minor, J. Mater. Res. **3**, 832 (1988).
[15]Y. Kubo, T. Ichihashi, T. Manako, K. Baba, J. Tabuchi, and H. Igarashi, Phys. Rev. B **37**, 7858 (1988).
[16]J. D. Jorgensen, W. B. Veal, W. K. Kwok, G. W. Crabtree, A. Umezawa, L. J. Nowicki, and A. P. Paulikas, Phys. Rev. B **36**, 5731 (1987).
[17]W. K. Kwok, G. W. Crabtree, A. Umezawa, B. W. Veal, J. D. Jorgensen, S. K. Malik, L. J. Nowicki, A. P. Paulikas, and L. Nunez, Phys. Rev. B **37**, 106 (1988).
[18]J. van den Berg, C. J. van der Beek, P. H. Kes, G. J. Nieuwenhuys, J. A. Mydosh, H. W. Zandbergen, F. P. F. van Berkel, R. Steens, and D. J. W. Ijdo, Europhys. Lett. **4**, 737 (1987).
[19]T. Gourieux, G. Krill, M. Maurer, M. F. Ravet, A. Menny, H. Tolentino, and A. Fontaine, Phys. Rev. B **37**, 7516 (1988).
[20]C. Namgung, J. T. S. Irvine, J. H. Binks, and A. R. West (unpublished); and (private communication).
[21]P. K. Gallagher, H. M. O'Bryan, S. A. Sunshine, and D. W. Murphy, Mater. Res. Bull. **22**, 995 (1987).
[22]H. M. O'Bryan and P. K. Gallagher, Adv. Ceram. Mater. **2**, 640 (1987).
[23]R. Beyers, G. Lim, E. M. Engler, V. Y. Lee, M. L. Ramirez, R. J. Savoy, R. D. Jacowitz, T. M. Shaw, S. La Placa, R. Boehme, C. C. Tsuei, Sung I. Park, M. W. Shafer, and W. J. Gallagher, Appl. Phys. Lett. **51**, 614 (1987).
[24]A. Manthiram, J. S. Swinnea, Z. T. Sui, H. Steinfink, and J. B. Goodenough, J. Am. Chem. Soc. **109**, 6667 (1987).
[25]K. Ikeda, M. Nagata, M. Ishihara, S. Kumazawa, T. Shibayama, A. Imagawa, T. Sugamata, H. Katoh, H. Momozawa, K. Umezawa, and K. Ishida, Jpn. J. Appl. Phys. **27**, L202 (1988).
[26]C. Namgung, J. T. S. Irvine, J. H. Binks, and A. R. West, Solid State Commun. (to be published).
[27]J. D Jorgensen, H. Shaked, D. G. Hinks, B. Dabrowski, B. W. Veal, A. P. Paulikas, L. J. Nowicki, G. W. Crabtree, W. K. Kwok, L. H. Nunez, and H. Claus, Physica **153-155C**, 578 (1988).
[28]W. I. F. David, W. T. A. Harrison, J. M. F. Gunn, O. Moze, A. K. Soper, P. Day, J. D. Jorgensen, M. A. Beno, D. W. Capone, D. G. Hinks, I. K. Schuller, L. Soderholm, C. U. Segre, K. Zhang, and J. D. Grace, Nature **327**, 310 (1987).
[29]J. J. Capponi, C. Chaillout, A. W. Hewat, P. Lejay, M. Marezio, N. Nguyon, B. Raveau, J. L. Soubeyroux, J. L. Tholence, and R. Tournier, Europhys. Lett. **3**, 1301 (1987).
[30]M.-H. Whangbo, M. Evain, M. A. Beno, Urs. Geiser, and J. M. Williams, Inorg. Chem. **27**, 467 (1988).
[31]P. F. Miceli, J. M. Tarascon, L. H. Greene, P. Barboux, F. J. Rotella, and J. D. Jorgensen, Phys. Rev. B **37**, 5932 (1988).
[32]A. Renault, J. K. Burdett, and J.-P. Pouget, J. Solid State Chem. **71**, 587 (1987).
[33]E. H. Appelman, L. R. Morss, A. M. Kini, U. Geiser, A. Umezawa, G. W. Crabtree, and K. D. Carlson, Inorg. Chem. **26**, 3237 (1987).
[34]D. N. Hume, I. M. Kolthoff, Ind. Eng. Chem. Anal. Ed. **16**, 103 (1944).
[35]K. Kishio *et al.*, Jpn. J. Appl. Phys. **26**, L1228 (1987).
[36]E. D. Specht, C. J. Sparks, A. G. Dhere, J. Brynestad, O. B. Cavin, D. M. Kroeger, and H. A. Oye, Phys. Rev. B **37**, 7426 (1988).
[37]P. K. Gallagher, Adv. Ceram. Mater. **2**, 632 (1987).
[38]P. Strobel, J. J. Capponi, and M. Marezio, Solid State Commun. **64**, 513 (1987).
[39]S. Yamaguchi, K. Terabe, A. Saito, S. Yahagi, and Y. Iguchi, Jpn. J. Appl. Phys. **27**, L179 (1988).
[40]T. B. Lindemer, J. F. Hunley, J. E. Gates, A. L. Sutton, Jr., J. Brynestad, C. R. Hubbard, and P. K. Gallagher, Oak Ridge National Laboratory Report No. ORNL/TM-10899 (1989) (unpublished); J. Amer. Ceram. Soc. **72**, 1775 (1989).
[41]G. W. Crabtree, B. W. Veal, W. K. Kwok, H. Claus, and L. H. Nunez (unpublished).
[42]J. D. Jorgensen, J. Faber, Jr., J. M. Carpenter, R. K. Crawford, J. F. Haumann, R. L. Hitterman, R. Kleb, G. E. Ostrowski, F. J. Rotella, and T. G. Worlton, J. Appl. Crystallogr. **22**, 321 (1989).
[43]R. B. VonDreele, J. D. Jorgensen, and C. G. Windsor, J. Appl. Crystallogr. **15**, 581 (1982).
[44]J. D. Jorgensen, M. A. Beno, D. G. Hinks, L. Soderholm, K. J. Volin, R. L. Hitterman, J. D. Grace, I. K. Schuller, C. E. Segre, K. Zhang, and M. S. Kleefisch, Phys. Rev. B **36**, 3608 (1987).
[45]A reanalysis of the data from Ref. 44 confirms that additional oxygen vacancies are present on the O(4) site and that the *O-T* transition occurs *in situ* near an oxygen content of 6.4.
[46]Y. Kubo, Y. Nakabayashi, J. Tabuchi, T. Yoshitake, A. Ochi, L. Utsumi, H. Igarashi, and M. Yonezawa, Jpn. J. Appl. Phys. **26**, L1888 (1987).
[47]A. T. Fiory, M. Gurvitch, R. J. Cava, and G. P. Espinosa, Phys. Rev. B **36**, 7262 (1987).
[48]P. P. Freitas and T. S. Plaskett, Phys. Rev. B **36**, 5723 (1987).
[49]M. Tetenbaum, B. Tani, B. Czech, and M. Blander, Physica **158C**, 377 (1989).
[50]R. Beyers, B. T. Ahn, G. Gorman, V. Y. Lee, S. S. P. Parkin,

M. L. Ramirez, K. P. Roche, J. E. Vazquez, T. M. Gur, and R. A. Huggins, Nature **340**, 619 (1989).

[51]H. Shaked, J. D. Jorgensen, J. Faber, Jr., D. G. Hinks, and B. Dabrowski, Phys. Rev. B **39**, 7363 (1989).

[52]C. C. Torardi, E. M. McCarron, M. A. Subramanian, H. S. Horowitz, J. B. Michel, A. W. Sleight, and D. E. Cox, in *Chemistry of High-Temperature Superconductors,* ACS Symposium Series, edited by D. L. Nelson, M. S. Whittingham, and T. F. George (American Chemical Society, Washington, D.C., 1987), p. 152.

[53]A. Santoro, S. Miraglia, F. Beech, S. A. Sunshine, D. W. Murphy, L. F. Schneemeyer, and J. V. Waszczak, Mater. Res. Bull. **22**, 1007 (1987).

[54]S. Miraglia, F. Beech, A. Santoro, D. Tran Qui, S. A. Sunshine, and D. W. Murphy, Mater. Res. Bull. **22**, 1733 (1987).

[55]F. Beech, S. Miraglia, A. Santoro, and R. S. Roth, Phys. Rev. B **35**, 8778 (1987).

[56]Z. Jirak, F. Pollert, A. Triska, and S. Vratislav, Phys. Status Solidi A **102**, K61 (1987).

[57]Y. Tokura, J. B. Torrance, T. C. Huang, and A. I. Nazzal, Phys. Rev. B **38**, 7156 (1988).

[58]J. D. Jorgensen, D. G. Hinks, H. Shaked, B. Dabrowski, B. W. Veal, A. P. Paulikas, L. J. Nowicki, G. W. Crabtree, W. K. Kwok, A. Umezawa, L. H. Nunez, and B. D. Dunlap, Physica **156-157B**, 877 (1989).

[59]D. B. Mitzi, P. T. Feffer, J. M. Newsam, D. J. Webb, P. Klavins, A. J. Jacobson, and A. Kapitulnik, Phys. Rev. B **38**, 6667 (1988).

[60]P. F. Miceli, J. M. Tarascon, L. H. Greene, P. Barboux, J. D. Jorgensen, J. J. Rhyne, and D. A. Neumann, in *Materials Research Society Symposium Proceedings, San Diego, 1989,* Proceedings of the Materials Research Society Meeting, Symposium M: High Temperature Superconductors: Relationships Between Properties, Structure, and Solid State Chemistry, edited by J. D. Jorgensen, K. Kitazawa, J. M. Tarascon, M. S. Thompson, and J. B. Torrance (Materials Research Society, Pittsburgh, 1989), Vol. 156, p. 119.

[61]J. D. Jorgensen, B. Dabrowksi, D. G. Hinks, and C. U. Segre (unpublished).

[62]Y. Maeno, T. Tomita, M. Kyogoku, S. Awaji, Y. Aoki, K. Hoshino, A. Minami, and T. Fujita, Nature **328**, 512 (1987).

[63]J. M. Tarascon, P. Barboux, P. F. Miceli, L. H. Greene, G. W. Hull, M. Eibschutz, and S. A. Sunshine, Phys. Rev. B **37**, 7458 (1988).

[64]R. J. Cava, B. Batlogg, R. M. Fleming, S. A. Sunshine, A. Ramirez, E. A. Rietman, S. M. Zahurak, and R. B. van Dover, Phys. Rev. B **37**, 5912 (1988).

[65]K. Takita, H. Akinaga, H. Katoh, H. Asano, and K. Masuda, Jpn. J. Appl. Phys. **27**, L67 (1988).

[66]H. Nozaki, S. Takehawa, and Y. Ishizawa, Jpn. J. Appl. Phys. **27**, L31 (1988).

[67]Z. Hiroi, M. Takano, Y. Takeda, R. Kanno, and Y. Bando, Jpn. J. Appl. Phys. **27**, L580 (1988).

[68]G. Roth, G. Heger, B. Renker, J. Pannetier, V. Caignaert, M. Hervieu, and B. Raveau, Z. Phys. B **71**, 43 (1988).

[69]J.-L. Hodeau, P. Bordet, J.-J. Capponi, C. Chaillout, and M. Marezio, Physica **153-155C**, 582 (1988).

[70]C. U. Segre, B. Dabrowski, D. G. Hinks, K. Zhang, J. D. Jorgensen, M. A. Beno, and I. K. Schuller, Nature **329**, 227 (1987).

[71]C. Chaillout, M. A. Alario-Franco, J. J. Capponi, J. Chenavas, J. L. Hodeau, and M. Marezio, Phys. Rev. B **36**, 7118 (1987).

[72]D. J. Werder, C. H. Chen, R. J. Cava, and B. Batlogg, Phys. Rev. B **37**, 2317 (1988).

[73]H. W. Zandbergen, G. VanTendeloo, T. Okabe, and S. Amelinckx, Phys. Status Solidi A **103**, 45 (1987).

[74]M. Tanaka, M. Terauchi, K. Tsuda, and A. Ono, Jpn. J. Appl. Phys. **26**, L1237 (1987).

[75]R. M. Flemming, L. F. Schneemeyer, P. K. Gallagher, B. Batlogg, L. W. Rupp, and J. V. Waszczak, Phys. Rev. B **37**, 7920 (1988).

[76]C. H. Chen, D. J. Werder, L. F. Schneemeyer, P. K. Gallagher, and J. V. Waszczak, Phys. Rev. B **38**, 2888 (1988).